EAI Endorsed Transactions
on Scalable Information Systems
Research Article EAI.EU

Secure Data Processing Technology of Distribution Network OPGW Line with Edge Computing

Ying Zeng[1,*], Zhongmiao Kang[1], Zhan Shi[1]

[1]Power dispatching control center of Guangdong Power Grid Co., Ltd, China (e-mail: yingzeng2022@126.com, zhongmiaokang@126.com, ZhanShiCSG@hotmail.com).

Abstract

Promoted by information technology and scalable information systems, the network design and communication method of optical fiber composite overhead ground wire (OPGW) have been in great progress recently. As the overhead transmission line has strict requirements on the outer diameter and weight of OPGW, it is of vital importance to perform the physical-layer secure data processing for the distribution network OPGW line with edge computing. To this end, we examine a physical-layer secure distribution network OPGW with edge computing in this article, where there exists one transmitter S, one receiver D, one authorized legitimate monitor LM, and an interfering node I. To better analyze the system performance, we firstly give the definition of the system outage probability, based on the secure data rate. Then, we evaluate the system performance for the distribution network OPGW, by deriving analytical outage probability of secure data processing, to facilitate the system performance evaluation of secure data processing in the entire SNR regime. Finally, we demonstrate some simulation results to validate the analytical results on the physical-layer secure distribution network OPGW line with edge computing.

Received on 02 November 2022; accepted on 15 December 2022; published on 11 January 2023

Keywords: Secrecy outage probability, OPGW communication, edge computing.

doi:10.4108/eetsis.v10i3.2837

1. Introduction

Promoted by information technology and scalable information systems [1–3], the network design and communication method of optical fiber composite overhead ground wire (OPGW) have been in great progress recently, where the overhead transmission line has strict requirements on the outer diameter and weight of OPGW [4, 5]. There are two feasible directions to increase the power communication capacity. One direction is to reduce the size of optical fiber and increase the capacity of fiber core in the optical fiber cable. The second direction is to reduce the loss of optical fiber and improve the communication capacity and transmission rate of single fiber. In order to adapt to the development of power communication, the research on two types of small size single-mode optical fiber and ultra-low loss G.654.E optical fiber has become a hot spot. In 2015, Corning released SMF-28 Ultra 200 optical fiber with an outer diameter of 245uM reduced to 200um. In 2019, Prysmian released BendBrightXS 180uM bend insensitive optical fiber, which is 50% smaller than traditional optical fiber, and compatible with G652 and G657 optical fiber standard. The OPGW used for ultra-high voltage is of stranded structure.

The OPGW made of 652.D optical fiber increases the number of optical fiber cores from 30 cores and 24 cores to 48 cores and 36 cores, respectively [6]. OPGW has excellent performance and provides a solution for power communication capacity expansion. However, the bending resistance of conventional G.652.D optical fiber is poor, and the micro bending loss after the coating is thinned deteriorates. Hence, it is necessary to study and design the G.652.D optical fiber, which has a better compatibility with a larger mode field bending resistant fiber. At the same time, the bending resistance of the fiber after the coating diameter should be reduced, which can further enhance the system performance of OPGW network.

*Corresponding author. Email: yingzeng2022@126.com

The G.654.E optical fiber for land use can reduce the attenuation while increasing the effective coverage, reduce the nonlinear effect, allow a larger input power, and achieve a longer distance for communication [7]. It has greater application advantages in remote areas and harsh environment with ultra high vacuum (UHV) communication. The transmission distance of single cross optical without relay is about 460km, and using G652 can no longer meet the requirements of longer distance, which imposes a serious challenge on the traditional communication system of ultra-long distance optical fiber. To solve this challenge, 8-core 130 with uM2 G.654 has been configured for the E optical fiber, and strict requirements on the G.654.E optical fiber has been put forward. After cabling, the average two-way average of single fiber at 1550nm wavelength is smaller than 0.165dB/km, which is far lower than the requirement in ITU-TG.654.E, where 1550nm attenuation is smaller than 0.23dB/km. However, lower attenuation means higher manufacturing cost, which needs to be combined with practical scenarios and new technologies of communication and computing.

Edge computing provides an effective solution to monitor the IoT based networks including the OPGW networks and 5G networks, where an intensive data analysis is involved [8, 9]. Due to limited computing resources such as limited computing frequency and limited energy supply, one single computing node may not calculate all of the computing tasks alone, where the edge computing has been proposed to accelerate the computing efficiently [10, 11]. In this area, many existing works have been performed to investigate the application of edge computing into the IoT based networks including the OPGW networks and 5G networks [12, 13]. For example, the computing latency can be effectively reduced by using the edge computing techniques, when the transmission quality of offloading the tasks is in good quality. In addition, the computing energy consumption can be also reduced effectively, when the offloading channel is in good condition, providing a good trade off between the computing and communication. Hence, it becomes an important task to investigate the effect of edge computing on the IoT based OPGW networks, especially the monitoring performance.

From the above literature review, we can find that it is of vital importance to perform the physical-layer secure data processing for the distribution network OPGW line with edge computing, where physical-layer security provides an effective solution to monitor the Internet of Things (IoT) based networks including the OPGW networks and 5G networks, in which an intensive data analysis is involved. Due to limited computing resources such as limited computing frequency and limited energy supply, one single computing node may not calculate all of the computing tasks alone, and accordingly edge computing is utilized for the transmission of OPGW networks. Hence, in this article, we examine a physical-layer secure distribution network OPGW with edge computing, where there exists a transmitter S, a receiver D, an authorized legitimate monitor LM, and an interfering node I. To better analyze the system performance, the definition of the system outage probability is firstly given based on the secure data rate difference between the main and monitoring links. Then, we evaluate the system performance for the distribution network OPGW, by deriving an analytical expression for the outage probability of secure data processing. Finally, the simulation results are demonstrated to show the validity of the analytical results on the physical-layer secure distribution network OPGW line with edge computing. The results in this work can provide some importance references for the development of information technology and scalable information systems.

.

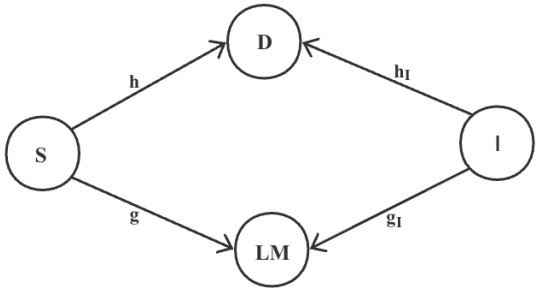

Figure 1. The system model of the secure data processing of distribution network OPGW line with edge computing, where there is one transmitter S, one destination D, one legitimate monitor LM and one interference node I.

2. System model of the secure data processing of distribution network OPGW line with edge computing

In this paper, we consider a secure distribution network OPGW line with edge computing, where there is one transmitter S, one receiver D which can act as the computing access node, one interference node I, and one authorized legitimate monitor LM. The transmitter S sends some intensive tasks to the edge node D via the wireless link for computing services, while the LM can monitor the data transmission in the network. In addition, the interference node I interferes with the wireless transmission of both data link and monitoring link. Specifically, let $h \sim \mathcal{CN}(0, \beta_1)$ and $g \sim \mathcal{CN}(0, \beta_2)$ denote the channel parameters from S to D and S to LM, respectively. In addition, $h_I \sim \mathcal{CN}(0, \beta_3)$ and $g_I \sim$

$\mathcal{CN}(0, \beta_4)$ are the channel parameters from I to D and I to LM, respectively. For the considered system, the received signal-to-noise ratios (SNRs) at D and LM are given by [14–16]

$$\mathrm{SNR_D} = \frac{P_S |h|^2}{P_I |h_I|^2}, \tag{1}$$

$$\mathrm{SNR_{LM}} = \frac{P_S |g|^2}{P_I |g_I|^2}, \tag{2}$$

where P_S is the transmit power at S and P_I is the interfering power at I. From (1) and (2), we can find that a larger P_I will deteriorate the received SNRs at D and LM, which leads to a poor data transmission performance as well as the monitoring performance.

2.1. Outage probability analysis on the secure data processing of distribution network OPGW line with edge computing

For the considered secure data processing of distribution network OPGW line with edge computing, we firstly give the definition of legitimate monitoring outage probability, which can help analyze and ensure the security of the system. The legitimate monitoring outage occurs when the instantaneous date rate of the monitoring link, i.e., $C_{SM} = log_2(1 + \mathrm{SNR_{LM}})$, falls below the instantaneous date rate of the data transmission, i.e., $C_{SD} = log_2(1 + \mathrm{SNR_D})$, given by [17, 18]

$$P_{out} = \Pr\left[C_{SM} - C_{SD} < Y^{th}\right], \tag{3}$$

According to (3), the legitimate monitoring outage happens if the data rate of the monitoring link is smaller than the transmission data rate. Hence, we can further write (3) as [19–21]

$$P_{out} = \Pr\left[\log_2(1 + \mathrm{SNR_{LM}}) - \log_2(1 + \mathrm{SNR_D}) < Y^{th})\right], \tag{4}$$

$$= \Pr\left[|Z_1|^2 < \left[A\left(1 + \frac{P_S}{P_I}|Z_2|^2\right) - 1\right]\frac{P_I}{P_S}\right], \tag{5}$$

where we use $A{=}2^{Y_{th}}$, $|Z_1|^2 = \frac{|h|^2}{|h_I|^2}$, and $|Z_2|^2 = \frac{|g|^2}{|g_I|^2}$ to simplify the notations. Since all the wireless channels experience Rayleigh flat fading, we can obtain the probability density functions (PDFs) of $|Z_1|^2$ and $|Z_2|^2$ as [22–24]

$$f_{|Z_1|^2} = \begin{cases} \frac{\beta_1\beta_3}{(\beta_1+\beta_3 y)^2}, & \text{If } y > 0 \\ 0, & \text{Else.} \end{cases}, \tag{6}$$

$$f_{|Z_2|^2} = \begin{cases} \frac{\beta_2\beta_4}{(\beta_2+\beta_4 x)^2}, & \text{If } x > 0 \\ 0, & \text{Else.} \end{cases}. \tag{7}$$

From (6) and (7), (5) can be rewritten as [25, 26]

$$P_{out} = \int_0^{+\infty}\int_0^{\left[A\left(1+\frac{P_S}{P_I}x\right)-1\right]\frac{P_I}{P_S}} \frac{\beta_1\beta_3}{(\beta_1+\beta_3 y)^2}\frac{\beta_2\beta_4}{(\beta_2+\beta_4 x)^2}dydx, \tag{8}$$

$$= \int_0^{+\infty} \frac{\beta_2\beta_4}{(\beta_2+\beta_4 x)^2}\left[1 - \frac{\beta_1}{\beta_1 + \beta_3[A(1+\frac{P_S}{P_I}x) - 1]\frac{P_I}{P_S}}\right]dx. \tag{9}$$

We can further derive P_{out} as

$$P_{out} = 1 - \int_0^{+\infty} \frac{\beta_1\beta_2\beta_4}{(\beta_2+\beta_4 x)^2\left[\beta_1 + A\beta_3 x + \frac{(A-1)\beta_3 P_I}{P_S}\right]}dx,$$

$$= 1 - \int_0^{+\infty} \frac{1}{k(1+ax)^2(1+bx)}dx, \tag{10}$$

where we use

$$k = \frac{\beta_1\beta_2 P_S + (A-1)\beta_2\beta_3 P_I}{\beta_1\beta_4 P_S}, \tag{11}$$

$$a = \frac{\beta_4}{\beta_2}, \tag{12}$$

$$b = \frac{A\beta_3 P_S}{\beta_1 P_S + (A-1)\beta_3 P_I}. \tag{13}$$

Then, we will discuss P_{out} for different relationships between a and b. Specifically, if $a = b$, we can have,

$$P_{out} = 1 - \int_0^{+\infty} \frac{1}{k(1+ax)^3}dx, \tag{14}$$

$$= 1 - \frac{1}{2ak}. \tag{15}$$

For the other case of $a \neq$ b, we can have

$$P_{out} = 1 - \int_0^{+\infty} \frac{1}{k}\left[\frac{b^2}{(b^2-2ab+a^2)(bx+1)} - \frac{ab}{(b^2-2ab+a^2)(ax+1)} - \frac{a}{(b-a)(ax+1)^2}\right]dx, \tag{16}$$

$$= 1 - \frac{b\ln(\frac{b}{a}) + a - b}{k(a-b)^2}. \tag{17}$$

By summarizing the analytical results in (15) and (17), one can readily perform the system performance evaluation of the secure data processing in the considered network.

3. Simulations on the secure data processing of distribution network OPGW line with edge computing

In this part, in order to verify the analytic results derived above, simulation results and analytical results

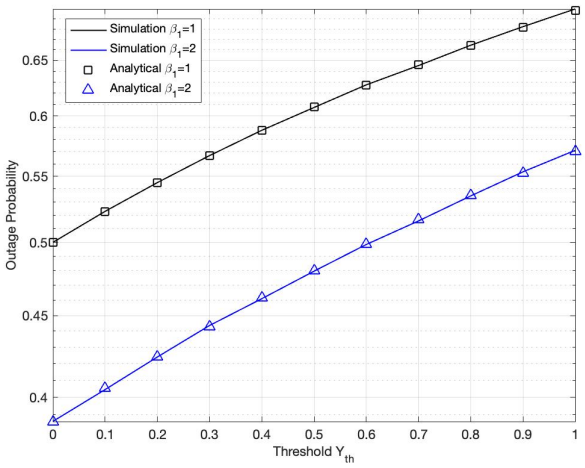

Figure 2. Impact of threshold Y_{th} on the system outage probability.

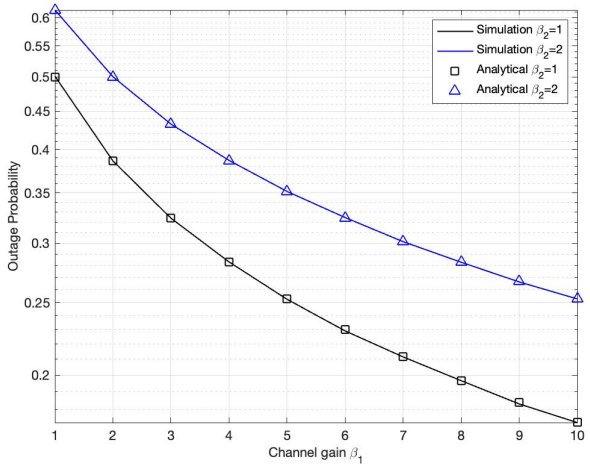

Figure 3. Impact of the average channel gain β_1 on the system outage probability.

are presented for the secure data processing of distribution network OPGW line with edge computing. In particular, the impact of parameters Y_{th}, β_1 and β_2 on the performance of the entire monitoring network is analyzed and simulated in the subsequent several figures. If we do not give the specific values, P_I, P_S, and Y_{th} are equal to 1W, 2W and 0, respectively, and the average channel gains β_1, β_2, β_3 and β_4 are all set to unity.

Fig. 2 illustrates the system outage probability with $\beta_1 = 1$ or 2 versus the threshold Y_{th}, where the threshold Y_{th} varies from 0bps to 1bps. As shown in Fig. 2, when $\beta_1 = 1$ or 2, the system outage probability increases with the increase of the threshold Y_{th}. For example, when $\beta_1 = 1$, the system outage probability with $Y_{th} = 0$ is about 0.5, while that with $Y_{th} = 1$ is about 0.7. When $\beta_1 = 2$, the system outage probability with $Y_{th} = 0$ is about 0.39, while that with $Y_{th} = 1$ is about 0.57. Moreover, we can also find that the average channel gain β_1 also affects the legitimate monitoring outage probability. In particular, the result with $\beta_1 = 2$ is smaller than that with $\beta_1 = 1$ when Y_{th} ranges in the interval of [0, 1]. In addition, the analytical P_{out} is almost equal to the simulation P_{out}. This validate the derived closed-form expressions for the legitimate monitoring outage probability. For example, the analytical outage probability with $\beta_1 = 2$ and $Y_{th} = 0.2$ is 0.4240, while the simulated outage probability with $\beta_1 = 2$ and $Y_{th} = 0.2$ is 0.4239, where the difference is only 0.0001. Such results verify the derived outage probability for the considered system.

Fig. 3 depicts the variation of the system outage probability with $\beta_2 = 1$ or 2 versus the average channel gain β_1, where the average channel gain β_1 varies in [1, 10]. As shown in Fig. 2, when $\beta_2 = 1$ or 2, the outage probability decreases with the increase of the channel gain of β_2. For example, the system outage probability with $\beta_1 = 1$ and $\beta_2 = 1$ is about 0.50, while the system outage probability with $\beta_1 = 10$ and $\beta_2 = 1$ is about 0.17. The system outage probability with $\beta_1 = 1$ and $\beta_2 = 2$ is about 0.61, while the system outage probability with $\beta_1 = 10$ and $\beta_2 = 2$ is about 0.25. This is because that increasing β_1 can help increase the corresponding SNR_D, which in turn leads to a lower legitimate monitoring outage probability. Moreover, we can also find that the channel gain β_2 also affects the legitimate monitoring outage probability. In particular, the system outage probability with $\beta_2 = 2$ is lower than that with $\beta_2 = 1$. In addition, the analytical P_{out} can match the simulation P_{out} well. This also validate the derived closed-form expressions for the system outage probability.

Fig. 4 presents the impact of the average channel gain β_2 on the system outage probability with $\beta_1 = 1$ or 2, where the average channel gain β_2 changes in [1, 10]. As shown in Fig. 4, when $\beta_1 = 1$ or 2, the system outage probability increases with the increasing channel gain β_2. In addition, increasing β_1 can effectively increase the corresponding SNR_LM, which in turn leads to a higher outage probability. For example, the system outage probability with $\beta_1 = 1$ and $\beta_2 = 1$ is about 0.50, while the system outage probability with $\beta_1 = 2$ and $\beta_2 = 1$ is about 0.39. The system outage probability with $\beta_1 = 1$ and $\beta_2 = 10$ is about 0.83, while the system outage probability with $\beta_1 = 2$ and $\beta_2 = 10$ is about 0.75. Moreover, we can also find that the average channel gain β_1 also affects the legitimate monitoring outage probability. Specifically, the value of P_{out} with $\beta_1 = 1$ is lower than that with $\beta_2 = 2$. In addition, the analytical P_{out} fits well with the simulated P_{out}. This further

Table 1 Numerical outage probability versus the threshold Y_{th}.

Y_{th}	0.0	0.2	0.4	0.6	0.8	1.0
Sim β_1=1	0.5000	0.5450	0.5877	0.6274	0.6643	0.6999
Ana β_1=1	0.5000	0.5450	0.5874	0.6272	0.6642	0.6985
Sim β_1=2	0.3864	0.4239	0.4611	0.4985	0.5347	0.5710
Ana β_1=2	0.3863	0.4240	0.4615	0.4986	0.5349	0.5703

Table 2 Numerical outage probability versus the average channel gain β_1.

β_1	1	3	5	7	9	10
Sim β_2=1	0.5012	0.3239	0.2525	0.2115	0.1830	0.1728
Ana β_2=1	0.5000	0.3240	0.2529	0.2117	0.1840	0.1732
Sim β_2=2	0.6141	0.4325	0.3517	0.3014	0.2663	0.2528
Ana β_2=2	0.6137	0.4328	0.3514	0.3015	0.2668	0.2529

Table 3 Numerical outage probability versus the channel gain β_2.

β_2	1	3	5	7	9	10
Sim β_1=1	0.5014	0.6745	0.7463	0.7888	0.8156	0.8274
Ana β_1=1	0.5000	0.6760	0.7471	0.7883	0.8160	0.8268
Sim β_1=2	0.3867	0.5661	0.6481	0.6986	0.7335	0.7473
Ana β_1=2	0.3863	0.5672	0.6486	0.6985	0.7332	0.7471

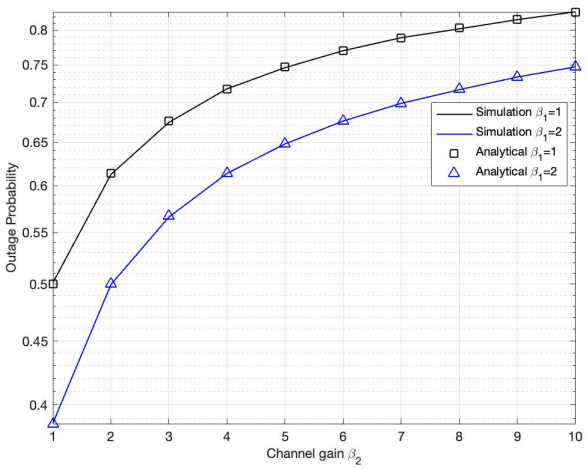

Figure 4. Impact of the average channel gain β_2 on the system outage probability.

validates the derived closed-form expressions for the system outage probability of the considered network.

4. Conclusions

In this paper, we investigate the secure data processing of distribution network OPGW line with edge computing, where the intensive tasks may be involved to perform the data analysis on the network maintenance. To assist the the system performance analysis, we firstly gave the definition of the system outage probability based on the secure data rate difference between the main and monitoring links. Then, we evaluated the system performance for the distribution network OPGW, by deriving an analytical expression for the outage probability of secure data processing. Finally, the simulation results were demonstrated to show the validity of the analytical results on the physical-layer secure distribution network OPGW line with edge computing. The results in this work could provide some importance

references for the development of information technology and scalable information systems.

5. Acknowledgements

This work was supported by Science and Technology Project of China Southern Power Grid 035300kk52190039 (No. gdkjxm20201993).

5.1. Data Availability Statement

The data of this work can be found through the email to: Ying Zeng(yingzeng2022@126.com), Zhongmiao Kang(zhongmiaokang@126.com), and Zhan Shi(ZhanShiCSG@hotmail.com).

5.2. Copyright

References

[1] Z. Na, C. Ji, B. Lin, and N. Zhang, "Joint optimization of trajectory and resource allocation in secure uav relaying communications for internet of things," *IEEE Internet of Things Journal*, 2022.

[2] Y. Wu and C. Gao, "Intelligent resource allocation scheme for cloud-edge-end framework aided multi-source data stream," *to appear in EURASIP J. Adv. Signal Process.*, vol. 2023, no. 1, 2023.

[3] R. Zhao and M. Tang, "Profit maximization in cache-aided intelligent computing networks," *Physical Communication*, vol. PP, no. 99, pp. 1–10, 2022.

[4] N. Dahlin and R. Jain, "Scheduling flexible nonpreemptive loads in smart-grid networks," *IEEE Trans. Control. Netw. Syst.*, vol. 9, no. 1, pp. 14–24, 2022.

[5] E. Z. Serper and A. Altin-Kayhan, "Coverage and connectivity based lifetime maximization with topology update for WSN in smart grid applications," *Comput. Networks*, vol. 209, p. 108940, 2022.

[6] Z. Alavikia and M. Shabro, "A comprehensive layered approach for implementing internet of things-enabled smart grid: A survey," *Digit. Commun. Networks*, vol. 8, no. 3, pp. 388–410, 2022.

[7] S. Mishra, "Blockchain-based security in smart grid network," *Int. J. Commun. Networks Distributed Syst.*, vol. 28, no. 4, pp. 365–388, 2022.

[8] X. Lai, "Outdated access point selection for mobile edge computing with cochannel interference," *IEEE Trans. Vehic. Tech.*, vol. 71, no. 7, pp. 7445–7455, 2022.

[9] J. Ling and C. Gao, "Dqn based resource allocation for NOMA-MEC aided multi-source data stream," *to appear in EURASIP J. Adv. Signal Process.*, vol. 2023, no. 1, 2023.

[10] S. Tang, "Dilated convolution based CSI feedback compression for massive MIMO systems," *IEEE Trans. Vehic. Tech.*, vol. 71, no. 5, pp. 211–216, 2022.

[11] S. Tang and L. Chen, "Computational intelligence and deep learning for next-generation edge-enabled industrial IoT," *IEEE Trans. Netw. Sci. Eng.*, vol. 9, no. 3, pp. 105–117, 2022.

[12] L. Chen, "Physical-layer security on mobile edge computing for emerging cyber physical systems," *Computer Communications*, vol. 194, no. 1, pp. 180–188, 2022.

[13] L. He and X. Tang, "Learning-based MIMO detection with dynamic spatial modulation," *IEEE Transactions on Cognitive Communications and Networking*, vol. PP, no. 99, pp. 1–12, 2023.

[14] B. Li, Z. Na, and B. Lin, "Uav trajectory planning from a comprehensive energy efficiency perspective in harsh environments," *IEEE Network*, vol. 36, no. 4, pp. 62–68, 2022.

[15] X. Zheng and C. Gao, "Intelligent computing for WPT-MEC aided multi-source data stream," *to appear in EURASIP J. Adv. Signal Process.*, vol. 2023, no. 1, 2023.

[16] W. Wu, F. Zhou, R. Q. Hu, and B. Wang, "Energy-efficient resource allocation for secure noma-enabled mobile edge computing networks," *IEEE Trans. Commun.*, vol. 68, no. 1, pp. 493–505, 2020.

[17] L. Zhang and C. Gao, "Deep reinforcement learning based IRS-assisted mobile edge computing under physical-layer security," *Physical Communication*, vol. 55, p. 101896, 2022.

[18] Y. Guo and W. Xu, "Resource allocation in wireless power transfer assisted federated learning networks," *IEEE Transactions on Communications*, vol. PP, no. 99, pp. 1–12, 2023.

[19] L. Chen and X. Lei, "Relay-assisted federated edge learning:Performance analysis and system optimization," *IEEE Transactions on Communications*, vol. PP, no. 99, pp. 1–12, 2022.

[20] W. Zhou and X. Lei, "Priority-aware resource scheduling for uav-mounted mobile edge computing networks," *IEEE Trans. Vehic. Tech.*, vol. PP, no. 99, pp. 1–6, 2023.

[21] J. Lu and M. Tang, "Performance analysis for IRS-assisted MEC networks with unit selection," *Physical Communication*, vol. 55, p. 101869, 2022.

[22] W. Zhou and F. Zhou, "Profit maximization for cache-enabled vehicular mobile edge computing networks," *IEEE Trans. Vehic. Tech.*, vol. PP, no. 99, pp. 1–6, 2023.

[23] Y. Wu and C. Gao, "Task offloading for vehicular edge computing with imperfect CSI: A deep reinforcement approach," *Physical Communication*, vol. 55, p. 101867, 2022.

[24] S. Tang and X. Lei, "Collaborative cache-aided relaying networks: Performance evaluation and system optimization," *IEEE Journal on Selected Areas in Communications*, vol. PP, no. 99, pp. 1–12, 2022.

[25] R. Zhao, C. Fan, J. Ou, D. Fan, J. Ou, and M. Tang, "Impact of direct links on intelligent reflect surface-aided mec networks," *Physical Communication*, vol. 55, p. 101905, 2022.

[26] W. Wu, F. Zhou, B. Wang, Q. Wu, C. Dong, and R. Q. Hu, "Unmanned aerial vehicle swarm-enabled edge computing: Potentials, promising technologies, and challenges," *IEEE Wirel. Commun.*, vol. 29, no. 4, pp. 78–85, 2022.